Classification of equilibrium solutions of the cometary flow equation and explicit solutions of the Euler equations for monatomic ideal gases

Klemens Fellner[1] and Christian Schmeiser[2]

Abstract. The set of smooth equilibrium solutions of a kinetic model for cometary flows is split into equivalence classes according to similarity transformations. For each equivalence class in the two- and three-dimensional cases a normal form is computed. Each such equilibrum solution gives rise to an explicit solution of the compressible Euler equations for monatomic gases. The set of these solutions is discussed with special emphasis on solutions containing vacuum regions.

Key words: Euler equations, cometary flows,

AMS subject classification:

Acknowledgment: This work has been supported by the Austrian Science Foundation (grant nos. W008 and P16174-N05) and by the EU funded HYKE network (contract no. HPRN-CT-2002-00282). The first author also acknowledges support from the Wittgenstein award project of Peter Markowich.

[1]Institute for Mathematics, University of Vienna, Austria.

[2]Institute for Analysis and Scientific Computing, Vienna University of Technology, Austria, and RICAM, Linz, Austria.

1 Introduction and main ideas

We consider the kinetic transport equation

$$\partial_t f + \mathbf{v}\cdot\nabla_{\mathbf{x}} f = Q(f) = \frac{1}{|S^{d-1}|}\int_{S^{d-1}} f(\mathbf{u}_f + |\mathbf{v}-\mathbf{u}_f|\boldsymbol{\omega})\, d\boldsymbol{\omega} - f, \qquad (1)$$

for a nonnegative particle distribution function $f(t,\mathbf{x},\mathbf{v})$ depending on time $t \in \mathbb{R}$, position x in a domain $\Omega \subset \mathbb{R}^d$, and velocity $\mathbf{v} \in \mathbb{R}^d$, $d \geq 1$, where S^{d-1} and $|S^{d-1}|$ denote the unit sphere in $\mathbb{R}^d$ and its surface, respectively. The collision operator $Q(f)$ is an approximative model for the scattering of cosmic rays (energetic particles) in an astrophysical plasma, caused by random irregularities in an ambient field [7, 12, 13, 14]. The collisions tend to isotropize the velocity distribution around the particle mean velocity $\mathbf{u}_f(t,\mathbf{x})$ which, together with the mass density $\rho_f(t,\mathbf{x})$ and the specific internal energy $e_f(t,\mathbf{x})$ is given by

$$\rho_f = \int_{\mathbb{R}^d} f\, d\mathbf{v}, \quad \rho_f\mathbf{u}_f = \int_{\mathbb{R}^d} \mathbf{v} f\, d\mathbf{v}, \quad \rho_f e_f = \int_{\mathbb{R}^d} \frac{|\mathbf{v}-\mathbf{u}|^2}{2} f\, d\mathbf{v}. \qquad (2)$$

More precisely, the null set of the collision operator Q consists of all distributions of the form $f(v) = F(|\mathbf{v}-\mathbf{u}|^2/2)$, where F is an arbitrary function of one variable and $\mathbf{u}$ an arbitrary vector. The collision invariants of Q are $\mathbf{v}$, and all functions of the form $\varphi(|\mathbf{v}-\mathbf{u}_f|^2/2)$. Among them, only 1, $\mathbf{v}$, and $|\mathbf{v}|^2 = |\mathbf{v}-\mathbf{u}_f|^2 + \mathbf{v}\cdot\mathbf{u}_f - |\mathbf{u}_f|^2$ are independent from the distribution function and, thus, lead to the macroscopic conservation laws of mass, momentum, and energy, respectively:

$$\begin{aligned} \partial_t\rho_f \quad &+ \quad \nabla_{\mathbf{x}}\cdot(\rho_f\mathbf{u}_f) = 0\,, \\ \partial_t(\rho_f\mathbf{u}_f) \quad &+ \quad \nabla_{\mathbf{x}}\cdot\left(\int_{\mathbb{R}^d}\mathbf{v}\otimes\mathbf{v} f\, d\mathbf{v}\right) = 0\,, \\ \partial_t\left(\rho_f e_f + \rho_f\frac{|\mathbf{u}_f|^2}{2}\right) \quad &+ \quad \nabla_{\mathbf{x}}\cdot\left(\int_{\mathbb{R}^d}\mathbf{v}\frac{|\mathbf{v}|^2}{2} f\, d\mathbf{v}\right) = 0\,. \end{aligned} \qquad (3)$$

The hydrodynamic limit of (1) (i.e. the limit $\varepsilon \to 0$ after rescaling $t \to t/\varepsilon$ and $\mathbf{x} \to \mathbf{x}/\varepsilon$) has been investigated in [3, 4]. Formally, the particle distribution converges to a function f_0 of the form

$$f_0(t,\mathbf{x},\mathbf{v}) = F\left(t,\mathbf{x},\frac{|\mathbf{v}-\mathbf{u}(t,\mathbf{x})|^2}{2}\right), \qquad (4)$$

and evolution equations for $F(t,\mathbf{x},\xi)$ and for $\mathbf{u}(t,\mathbf{x})$ can be given. Essential for the results of this work is the observation that these evolution equations contain the above conservation laws as a closed subsystem, i.e., for distribution functions of the form (4), the momentum and energy fluxes can be computed in terms of the mass, momentum, and energy densities:

$$\int_{\mathbb{R}^d} \mathbf{v}\otimes\mathbf{v}F\,d\mathbf{v} = \rho_F\mathbf{u}_F\otimes\mathbf{u}_F + p_F\,\mathrm{Id}\,,$$

$$\int_{\mathbb{R}^d} \mathbf{v}\frac{|\mathbf{v}|^2}{2}F\,d\mathbf{v} = \rho_F\mathbf{u}_F\left(e_F + \frac{|\mathbf{u}_F|^2}{2}\right) + p_F\mathbf{u}_F\,,$$

with $p_F = (\gamma-1)\rho_F e_F$ and $\gamma = (d+2)/d$. With these closure relations, (3) are the compressible Euler equations for a monatomic gas. Other basic equations of fluid mechanics, such as the incompressible Navier-Stokes equations, are also contained in (1) as a singular limit [10]. For an existence theory see [5, 8].

The other crucial ingredient of this work is the identification of all smooth equilibrium solutions of (1) carried out in [8], where an equilibrium solution is a solution of (1) satisfying

$$\partial_t f + \mathbf{v}\cdot\nabla_{\mathbf{x}} f = Q(f) = 0\,. \tag{5}$$

In [8], the motivation for studying (5) was the long time behaviour of solutions of (1). Here we are particularly interested in exploring the fact that solutions of (5) give rise to solutions of the compressible Euler equations.

The results of [8] correspond to those of Desvillettes [6] for the gas dynamics Boltzmann equation. Every smooth solution of (5) can be written in the form

$$f(t,\mathbf{x},\mathbf{v}) = \psi\left(\alpha(t)\xi(t,\mathbf{x},\mathbf{v}) + g(t,\mathbf{x})\right), \tag{6}$$

with

$$\alpha(t) = at^2 + 2bt + c\,, \tag{7}$$

$$\xi(t,\mathbf{x},\mathbf{v}) = \frac{1}{2}|\mathbf{v}-\mathbf{u}(t,\mathbf{x})|^2\,, \tag{8}$$

$$\begin{aligned} g(t,\mathbf{x}) = {} & \frac{1}{2\alpha(t)}\mathbf{x}^T\left(ac-b^2+\Lambda^2\right)\mathbf{x} \\ & + \left(\mathbf{A} + \frac{1}{\alpha(t)}(\Lambda - at - b)(\mathbf{A}t+\mathbf{B})\right)\cdot\mathbf{x} \\ & - \frac{1}{2\alpha(t)}|\mathbf{A}t+\mathbf{B}|^2\,, \end{aligned} \tag{9}$$

$$\mathbf{u}(t,\mathbf{x}) = \frac{1}{\alpha(t)}\left(\Lambda\mathbf{x} + (at+b)\mathbf{x} + \mathbf{A}t + \mathbf{B}\right)\,. \tag{10}$$

In (6)–(10), ψ is an arbitrary function of one variable. Also the scalars $a, b, c \in \mathbb{R}$, the vectors $\mathbf{A}, \mathbf{B} \in \mathbb{R}^d$, and the skew symmetric matrix $\Lambda \in \mathbb{R}^{d\times d}$ can be chosen arbitrarily. The gas dynamics case is included with $\psi = \exp$. Here, also compactly supported ψ can be chosen, giving rise to solutions including vacuum regions.

From (6), (8) it is obvious that $Q(f) = 0$ holds. On the other hand, the argument of ψ can also be written as

$$\begin{aligned}\alpha(t)\xi(t,\mathbf{x},\mathbf{v}) + g(t,\mathbf{x}) &= \frac{a}{2}|\mathbf{x}-\mathbf{v}t|^2 - b\mathbf{v}\cdot(\mathbf{x}-\mathbf{v}t) + \frac{c}{2}|\mathbf{v}|^2 \\ &\quad + \mathbf{A}\cdot(\mathbf{x}-\mathbf{v}t) - \mathbf{B}\cdot\mathbf{v} - \mathbf{v}^T\Lambda(\mathbf{x}-\mathbf{v}t)\,,\end{aligned}$$

showing that f also solves the free transport equation $\partial_t f + \mathbf{v}\cdot\nabla_{\mathbf{x}} f = 0$ (since it depends on t and $\mathbf{x}$ only in the combination $\mathbf{x} - \mathbf{v}t$).

For the computation of moments of distributions of the form (6)–(10), the behaviour of $\alpha(t)$ has to be taken into account. At zeroes of $\alpha(t)$, the distribution is independent from the velocity and moments do not exist in general. Therefore we restrict the following discussion to time intervals where $\alpha(t)$ does not change sign and assume $\alpha(t) > 0$. This is no restriction since the sign of $\alpha(t)$ can be absorbed in the definition of ψ. All moments up to the energy flux can then be computed if ψ decays sufficiently fast, such that integrals of the form $\int_{\eta_0}^{\infty} \eta^{(d+1)/2}\psi(\eta)d\eta$ exist. In particular, a straightforward computation gives

$$\rho(t,\mathbf{x}) = -\alpha(t)^{-d/2}\varphi'(g(t,\mathbf{x}))\,, \quad (\rho T)(t,\mathbf{x}) = \alpha(t)^{-1-d/2}\varphi(g(t,\mathbf{x}))\,,$$

for the temperature $T = \frac{2}{d}e$, with

$$\varphi(g) = \frac{|S^{d-1}|}{d}\int_0^{\infty}(2\eta)^{d/2}\psi(\eta+g)d\eta\,. \tag{11}$$

It is easily checked that ρ and T, together with the velocity $\mathbf{u}$ given by (10) solve the compressible Euler equations for an arbitrary decreasing profile φ, not necessarily coming from a kinetic profile ψ through (11). This provides a large class of explicit solutions for the compressible Euler equations.

The outline of the rest of the paper is the following: In section 2, we classify the set of equilibria (6) − (10) for $d = 2, 3$ according to the rank of the matrix in the quadratic form (9). More precisely, we identify equivalence classes under the symmetry group of the Euler equations (contained in the symmetry group of the cometary flow equation). For each equivalence class a normal form is given.

The classification for $d = 3$ is visualized in terms of the geometry and the dynamics of the level sets of the function $g(t, \cdot)$ in section 3. In particular, for profiles φ with compact support these level sets can be boundaries of vacuum regions.

In section 4, the map (11) from the kinetic profile ψ to the macroscopic profile φ is inverted. Finally, several types of explicit solutions for the 3D compressible Euler equations are discussed in section 5.

2 Classification of equilibrium solutions

The compressible Euler equations, the cometary flow equation, and the class (6)–(10) of equilibrium solutions are invariant under shifts in time and position, under Galilei transformations, under rotations and under certain rescalings of position and time. In the following we list the corresponding transformations and their effect on the parameters $a, b, c, \mathbf{A}, \mathbf{B}, \Lambda$ in (7), (9), and (10).

S1. Time shift The transformation $t \to t+t_0$ leaves the parameters $a, \mathbf{A}, \Lambda$ unchanged and leads to

$$b \to b + at_0\,, \quad c \to c + 2bt_0 + at_0^2\,, \quad \mathbf{B} \to \mathbf{B} + \mathbf{A}t_0\,.$$

S2. Galilei We combine a shift in position with a Galilei transformation in $\mathbf{x} \to \mathbf{x} + \mathbf{x}_0 + \mathbf{v}_0 t$, $\mathbf{v} \to \mathbf{v} + \mathbf{v}_0$, $\mathbf{u} \to \mathbf{u} + \mathbf{v}_0$. This leaves a, b, c, Λ unchanged and leads to

$$\mathbf{A} \to \mathbf{A} + a\mathbf{x}_0 + (\Lambda - b)\mathbf{v}_0\,, \quad \mathbf{B} \to \mathbf{B} + (\Lambda + b)\mathbf{x}_0 - c\mathbf{v}_0\,.$$

S3. Rotation The transformation $\mathbf{x} \to R\mathbf{x}$, $\mathbf{v} \to R\mathbf{v}$ with $R^{-1} = R^T$ leaves a, b, c unchanged and leads to

$$\mathbf{A} \to R^T\mathbf{A}\,, \quad \mathbf{B} \to R^T\mathbf{B}\,, \quad \Lambda \to R^T \Lambda R\,.$$

S4. Rescaling The transformation $(t, \mathbf{x}, \mathbf{v}) \to (k_2 t, k_1 k_2 \mathbf{x}, k_1 \mathbf{v})$ with $k_1, k_2 \in \mathbb{R}\backslash\{0\}$ leads to

$$a \to k_1^2 k_2^2 a\,, \quad b \to k_1^2 k_2 b\,, \quad c \to k_1^2 c\,,$$

$$\mathbf{A} \to k_1 k_2 \mathbf{A}\,, \quad \mathbf{B} \to k_1 \mathbf{B}\,, \quad \Lambda \to k_1^2 k_2 \Lambda\,.$$

From now on, 'invariant' means 'invariant under transformations of the forms S1–S4'. In the following, the above transformations will be used to simplify (6)–(10). As an example, we consider the case, where the matrix

$ac - b^2 + \Lambda^2$ in the quadratic form g (see (9)) is invertible (an invariant property). Then after the transformation S2 with

$$\begin{aligned} \mathbf{x}_0 &= -(ac - b^2 + \Lambda^2)^{-1}(c\mathbf{A} + (\Lambda - b)\mathbf{B}) \,, \\ \mathbf{v}_0 &= -(ac - b^2 + \Lambda^2)^{-1}((\Lambda + b)\mathbf{A} - a\mathbf{B}) \,, \end{aligned}$$

we have $\mathbf{A} = \mathbf{B} = 0$. Now we consider the two- and three-dimensional situations in more detail.

The three-dimensional case

Our main classification criterion is the invariant rank of the matrix $ac - b^2 + \Lambda^2$. We start with the invertible case $\operatorname{rank}(ac - b^2 + \Lambda^2) = 3$. As mentioned above, a S2-transformation can be used to eliminate $\mathbf{A}$ and $\mathbf{B}$. The second step is a rotation (S3) to change the skew-symmetric matrix into

$$\Lambda = \begin{pmatrix} 0 & 0 & 0 \\ 0 & 0 & \lambda \\ 0 & -\lambda & 0 \end{pmatrix} \,, \qquad (12)$$

such that the matrix-vector product can be written as $\Lambda\mathbf{x} = \mathbf{x} \times \mathbf{L}$ with $\mathbf{L} = (\lambda, 0, 0)$. It is easily seen that (in 3D) the invertibility of $ac - b^2 + \Lambda^2$ is equivalent to $0 \neq ac - b^2 \neq \lambda^2$.

For the next step we split into two subcases: If $a \neq 0$ holds (another invariant property), then we use a time shift (S1 with $t_0 = -b/a$) to eliminate b. Then $c \neq 0$ holds by the invertibility of $ac - b^2 + \Lambda^2$. Finally, a rescaling (S4) can be used to produce $a = 1$ and $|c| = 1$.

In the other subcase $a = 0$, $b \neq 0$ follows from the invertibility of $ac - b^2 + \Lambda^2$. Now a time shift (S1 with $t_0 = -c/b$) eliminates c, and a rescaling produces $b = 1$.

In both cases, a common factor is absorbed into the profile ψ to make α positive.

We have produced the first two normal forms:

Normal form type 3a: parameters: $\lambda \in \mathbb{R}$, $|c| = 1$, $c \neq \lambda^2$

$$\begin{aligned} \alpha(t) &= |t^2 + c| \,, \\ g(t, \mathbf{x}) &= \frac{cx_1^2 + (c - \lambda^2)(x_2^2 + x_3^2)}{2|t^2 + c|} \,, \\ \mathbf{u}(t, \mathbf{x}) &= \frac{t\mathbf{x} + \mathbf{x} \times \mathbf{L}}{t^2 + c} \,, \qquad \mathbf{L} = (\lambda, 0, 0) \,. \end{aligned}$$

Normal form type 3b: parameter: $\lambda \in \mathbb{R}$

$$\begin{aligned}
\alpha(t) &= 2|t|\,, \\
g(t,\mathbf{x}) &= \frac{-x_1^2 - (1+\lambda^2)(x_2^2+x_3^2)}{4|t|}\,, \\
\mathbf{u}(t,\mathbf{x}) &= \frac{\mathbf{x} + \mathbf{x}\times\mathbf{L}}{2t}\,, \qquad \mathbf{L} = (\lambda, 0, 0)\,.
\end{aligned}$$

The next case is $\mathrm{rank}(ac - b^2 + \Lambda^2) = 2$, implying $ac - b^2 = 0$ and $\Lambda \neq 0$. We start with a rotation to put Λ into the form (12). With a Galilei transformation (S2) we now cannot eliminate the vector parameters completely, but we can achieve $A_2 = A_3 = B_2 = B_3 = 0$.

Now we have again two subcases. When $a \neq 0$, we can use the first component of the Galilei transformation for $A_1 = 0$. With a time shift we produce $b = 0$ and, thus, $c = 0$ (because of $ac = b^2$). Finally, by rescaling and by absorbing a common factor into the profile ψ, we obtain $a = 1$ and $B_1 \in \{0, 1\}$.

In the second subcase $a = 0$, $b = 0$ follows and, thus, $c \neq 0$ (since $\alpha(t)$ would be identically equal to zero otherwise). Now, we produce $B_1 = 0$ with the first component of the Galilei transformation, and use rescaling as above for $c = 1$ and $A_1 \in \{0, 1\}$.

Normal form type 2a: parameters: $\lambda \neq 0$, $B_1 \in \{0, 1\}$

$$\begin{aligned}
\alpha(t) &= t^2\,, \\
g(t,\mathbf{x}) &= -\frac{\lambda^2(x_2^2+x_3^2) + B_1(1+2tx_1)}{2t^2}\,, \\
\mathbf{u}(t,\mathbf{x}) &= \frac{t\mathbf{x} + \mathbf{x}\times\mathbf{L} + (B_1, 0, 0)}{t^2}\,, \qquad \mathbf{L} = (\lambda, 0, 0)\,.
\end{aligned}$$

Normal form type 2b: parameters: $\lambda \neq 0$, $A_1 \in \{0, 1\}$

$$\begin{aligned}
\alpha(t) &= 1\,, \\
g(t,\mathbf{x}) &= -\lambda^2(x_2^2+x_3^2) + A_1(x_1 - t^2/2)\,, \\
\mathbf{u}(t,\mathbf{x}) &= \mathbf{x}\times\mathbf{L} + t(A_1, 0, 0)\,, \qquad \mathbf{L} = (\lambda, 0, 0)\,.
\end{aligned}$$

If $\mathrm{rank}(ac - b^2 + \Lambda^2) = 1$ holds, then we again start with a rotation to obtain (12). Then $0 \neq ac - b^2 = \lambda^2$ (implying $ac > 0$) holds. With a Galilei transformation $\mathbf{A} = B_1 = 0$ can be achieved. A time shift produces $b = 0$, and a rescaling leads to $a = c = 1$ and $|\mathbf{B}| \in \{0, 1\}$.

Normal form type 1: parameters: $|\lambda| = 1$, $B_2^2 + B_3^2 \in \{0,1\}$

$$\begin{aligned}
\alpha(t) &= t^2 + 1\,,\\
g(t,\mathbf{x}) &= \frac{x_1^2 + 2(\lambda B_3 - tB_2)x_2 - 2(\lambda B_2 + tB_3)x_3 - B_2^2 - B_3^2}{2(t^2+1)}\,,\\
\mathbf{u}(t,\mathbf{x}) &= \frac{t\mathbf{x} + \mathbf{x}\times\mathbf{L} + (0, B_2, B_3)}{t^2+1}\,, \qquad \mathbf{L} = (\lambda, 0, 0)\,.
\end{aligned}$$

Finally, the situation is left where the matrix $ac - b^2 + \Lambda^2$ vanishes and, thus, $ac - b^2 = \Lambda = 0$.

In the subcase $a \neq 0$, a time shift produces $b = 0$ and, as a consequence, $c = 0$. With a Galilei transformation we eliminate $\mathbf{A}$ and with a rotation $\mathbf{B} = (B_1, 0, 0)$ is obtained. A rescaling gives $a = 1$ and $B_1 \in \{0,1\}$.

For $a = 0$, $b = 0$ and $c \neq 0$ follow as for the type 2b. Now $\mathbf{B} = 0$ and $\mathbf{A} = (A_1, 0, 0)$ are the result of a Galilei transformation and of a rotation, respectively. Rescaling gives $c = 1$ and $A_1 \in \{0,1\}$.

Normal form type 0a: parameter: $B_1 \in \{0,1\}$

$$\begin{aligned}
\alpha(t) &= t^2\,,\\
g(t,\mathbf{x}) &= -\frac{B_1(1 + 2tx_1)}{2t^2}\,,\\
\mathbf{u}(t,\mathbf{x}) &= \frac{\mathbf{x}}{t} + \frac{1}{t^2}(B_1, 0, 0)\,.
\end{aligned}$$

Normal form type 0b: parameter: $A_1 \in \{0,1\}$

$$\begin{aligned}
\alpha(t) &= 1\,,\\
g(t,\mathbf{x}) &= A_1(x_1 - t^2/2)\,,\\
\mathbf{u}(t,\mathbf{x}) &= t(A_1, 0, 0)\,.
\end{aligned}$$

Actually, these last two types could be included in types 2a and 2b, repectively, by permitting $\lambda = 0$ there.

The two-dimensional case

Now the skew symmetric matrix always has the form

$$\Lambda = \begin{pmatrix} 0 & \lambda \\ -\lambda & 0 \end{pmatrix}\,,$$

and we have $ac - b^2 + \Lambda^2 = (ac - b^2 - \lambda^2)\mathrm{Id}$. Thus, there are only two cases concerning the rank of this matrix. If the rank is two, $\mathbf{A}$ and $\mathbf{B}$ are eliminated by a Galilei transformation.

In the first subcase $a \neq 0$, a time shift produces $b = 0$ and rescaling as well as absorption of a factor into ψ leads to $a = 1$, $c \in \{0, 1, -1\}$, $\lambda \in \{0, 1\}$.

For $a = 0$, $b \neq 0$, we achieve $c = 0$ by a time shift, and $b = 1$ by absorption of a factor.

In the third subcase $a = b = 0$, $c \neq 0$, we can obtain $c = 1$, $\lambda = 1$.

Normal form type 2a: parameters: $c \in \{0, 1, -1\}$, $\lambda \in \{0, 1\}$, $c \neq \lambda^2$

$$\begin{aligned} \alpha(t) &= t^2 + c\,, \\ g(t, \mathbf{x}) &= \frac{(c - \lambda^2)|x|^2}{2(t^2 + c)}\,, \\ \mathbf{u}(t, \mathbf{x}) &= \frac{t\mathbf{x} + \Lambda\mathbf{x}}{t^2 + c}\,. \end{aligned}$$

Normal form type 2b: parameter: $\lambda \in \mathbb{R}$

$$\begin{aligned} \alpha(t) &= 2t\,, \\ g(t, \mathbf{x}) &= -\frac{(1 + \lambda^2)|x|^2}{4t}\,, \\ \mathbf{u}(t, \mathbf{x}) &= \frac{\mathbf{x} + \Lambda\mathbf{x}}{2t}\,. \end{aligned}$$

Normal form type 2c:

$$\begin{aligned} \alpha(t) &= 1\,, \\ g(t, \mathbf{x}) &= -\frac{|x|^2}{2}\,, \\ \mathbf{u}(t, \mathbf{x}) &= \Lambda\mathbf{x}\,, \quad \Lambda = \begin{pmatrix} 0 & 1 \\ -1 & 0 \end{pmatrix}. \end{aligned}$$

For $ac - b^2 = \lambda^2$, we have two subcases: For $a \neq 0$, we get $\mathbf{A} = 0$ (Galilei), $\mathbf{B} = (B_1, 0)$ (rotation), $b = 0$ (time shift), $a = 1$, $c \in \{0, 1, -1\}$, $B_1 \in \{0, 1\}$ (rescaling, absorption).

Finally, $a = 0$ implies $b = \lambda = 0$, $c \neq 0$. We then obtain $\mathbf{B} = 0$ (Galilei), $\mathbf{A} = (A_1, 0)$ (rotation), $c = 1$, $A_1 \in \{0, 1\}$ (rescaling).

Normal form type 0a: parameters: $c \in \{0,1\}$, $B_1 \in \{0,1\}$, $\lambda^2 = c$

$$\begin{aligned}\alpha(t) &= t^2 + c\,,\\ g(t,\mathbf{x}) &= -\frac{B_1(1+2tx_1+2\lambda x_2)}{2(t^2+c)}\,,\\ \mathbf{u}(t,\mathbf{x}) &= \frac{t\mathbf{x}+\Lambda\mathbf{x}+(B_1,0)}{t^2+c}\,.\end{aligned}$$

Normal form type 0b: parameter: $A_1 \in \{0,1\}$

$$\begin{aligned}\alpha(t) &= 1\,,\\ g(t,\mathbf{x}) &= A_1(x_1 - t^2/2)\,,\\ \mathbf{u}(t,\mathbf{x}) &= t(A_1,0)\,.\end{aligned}$$

3 Visualization of 3D vacuum regions

We remark that the equilibrium distributions $F(t,\xi,\mathbf{x}) = \psi(\alpha(t)\xi + g(t,\mathbf{x}))$ depend on $\mathbf{x}$ only through $g(t,\mathbf{x})$. We therefore visualize the level sets

$$G(g_0,t) := \left\{\mathbf{x} \in \mathbb{R}^d : g(t,\mathbf{x}) \equiv g_0\right\}\,.$$

In particular, for compactly supported ψ, where $\psi(g) \equiv 0$ if $g \geq g_{vac}$ and supposing $\alpha(t) > 0$, the equilibria $F(t,\xi,\mathbf{x})$ feature a region of vacuum with boundary $G(g_{vac})$. The subsequently discussed figures Fig. 1.1– Fig. 2.2 show $G(g_0,t_1)$ and $G(g_0,t_2)$ for $t_1 < t_2$, where $G(g_0,t_1)$ is drawn in the brightest greylevel and $G(g_0,t_2)$ is colored the darkest towards the possible direction of vacuum.

Remark 3.1 ***(3D normal form type 3a: hyperboloids, ellipsoids)*** *The level sets $G(g_0,t)$ are either hyperboloids for $\lambda^2 > c = 1$ (Fig. 1.1, Fig. 1.2) or ellipsoids for $\lambda^2 < c = 1$ (Fig. 1.3) and for $c = -1$ (Fig. 1.4). Fig. 1.1 shows expanding vacuum due to strong rotation around the x_1 axis. In Fig. 1.2 rotating particles expanding from the center pushing the vacuum aside. In Fig. 1.3 the particles spread out into all directions. Fig. 1.4 for the case $c = -1$ shows an ellipsoid of expanding vacuum. The outgoing velocities origins from a singularity at time $t = 1$.*

Remark 3.2 ***(3D normal form type 2a: paraboloids, cylinders)*** *The level sets $G(g_0,t)$ are paraboloids or cylinders if, especially, $B_1 = 0$ or $A_1 = 0$ in type 2a or type 2b, respectively. As example, see figure Fig. 2.1 for cylindrically rotating particles with vacuum possibly inside.*

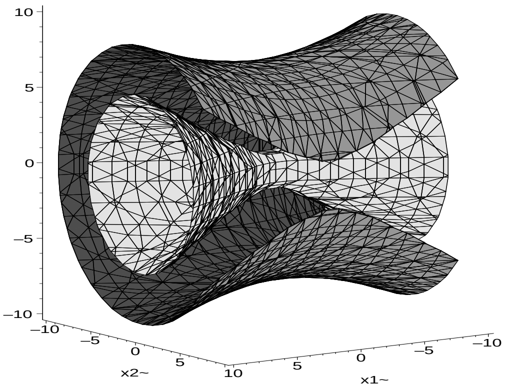

Fig. 1.1: Hyperboloid $G(-6, t)$ for normal from type 3a with $\lambda = 2, c = 1, t_1 = 0, t_2 = 5$

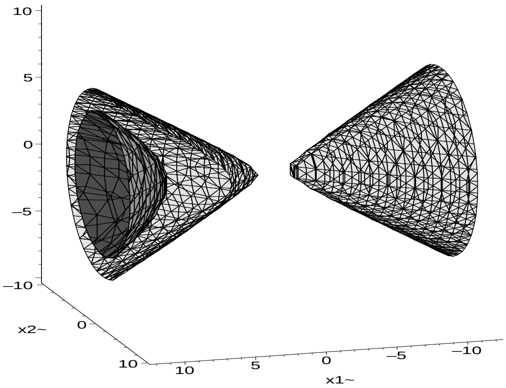

Fig. 1.2: Hyperboloid $G(1, t)$ for normal from type 3a with $\lambda = 2, c = 1, t_1 = 0, t_2 = 7.5$

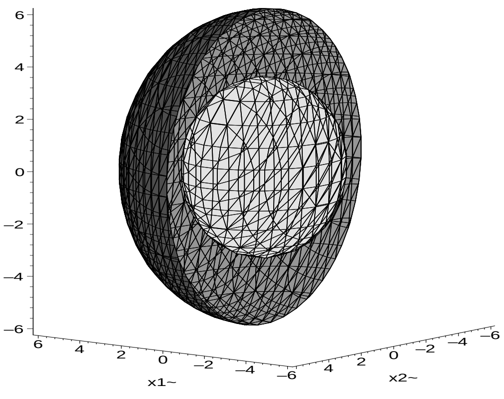

Fig. 1.3: Ellipsoid $G(9, t)$ for normal from type 3a with $\lambda = 0.5, c = 1, t_1 = 0, t_2 = \sqrt{2}$

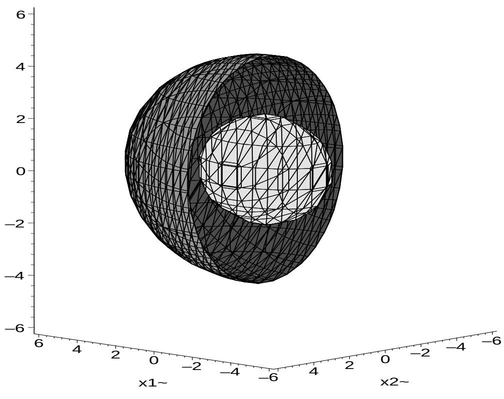

Fig. 1.4: Ellipsoid $G(-20, t)$ for normal from type 3a with $\lambda = 1, c = -1, t_1 = 1.2, t_2 = 1.7$

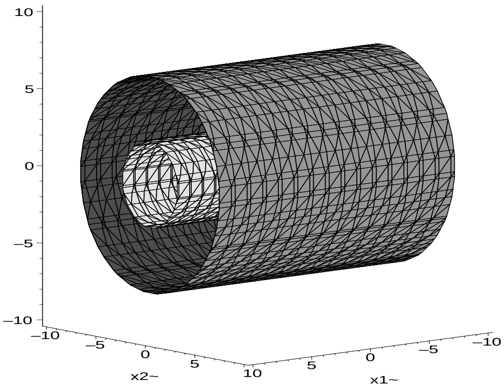

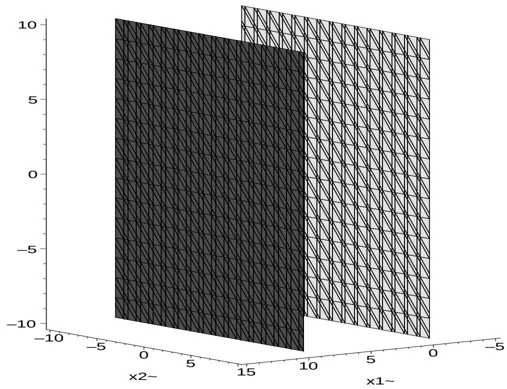

Fig. 2.1: Cylinder $G(-2,t)$ for normal form type 2a) with $\lambda = 1, B_1 = 0, t_1 = 2, t_2 = 5$

Fig. 2.2: Planes $G(0,t)$ for normal from type 0b) with $A_1 = 2$ at times $t_1 = 0, t_2 = 4.5$

Remark 3.3 ***(3D Example Normal form type 0b: planes)***
Figure Fig. 2.2 shows $G(g_0,t)$ as travelling planar fronts of particles.

4 Kinetic profiles from macroscopic profiles

This section is concerned with the inversion of the relation (11) between microscopic and macroscopic equilibrium profiles.

Lemma 4.1 *Let $\psi \in C(\mathbb{R})$ satisfy $\int_{\xi_0}^\infty |\xi|^{d/2}|\psi(\xi)|d\xi < \infty$ for a $d \in \mathbf{N}$ and a (and, thus, all) $\xi_0 \in \mathbb{R}$. Let φ be defined by (11). Then, for d even, $\varphi \in C^{d/2+1}(\mathbb{R})$ and*

$$\psi(\xi) = \frac{1}{c_d}\varphi^{(d/2+1)}(\xi) \qquad \textit{with } c_d = (-1)^{d/2+1}|S^{d-1}| \prod_{j=1}^{d/2-1}(d-2j)\,.$$

For d odd, $\varphi \in C^{(d+1)/2}(\mathbb{R})$ and

$$\psi(\xi) = \frac{1}{c_d}\frac{d}{d\xi}\int_\xi^\infty \varphi^{((d+1)/2)}(g)\frac{dg}{\sqrt{g-\xi}} \tag{13}$$
$$\textit{with } c_d = \frac{\pi}{\sqrt{2}}(-1)^{(d-1)/2}|S^{d-1}| \prod_{j=1}^{(d-1)/2}(d-2j)\,.$$

Proof: Doing k times a differentiation of (11) followed by an integration by parts, we obtain

$$\varphi^{(k)}(g) = (-1)^k |S^{d-1}| \prod_{j=1}^{(k-1)/2} (d-2j) \int_0^\infty (2\eta)^{d/2-k} \psi(\eta+g) d\eta \,.$$

Thus, the claim for d even follows with $k = d/2$ and then one more differentiation. For d odd, $k = (d+1)/2$ gives

$$\varphi^{((d+1)/2)}(g) = -\frac{c_d}{\pi} \int_g^\infty \frac{\psi(\xi)}{\sqrt{\xi - g}} d\xi \,.$$

This is an integral equation of Abel type for ψ, which can be solved explicitly (see, e.g., [9]) giving (13). □

Remark 4.1 *It is interesting to note that nonnegativity of ψ implies nonnegativity of φ, but not vice versa. On the other hand, the much stronger property of* complete monotonicity *($\varphi \in C^\infty(\mathbb{R})$ and $(-1)^k \varphi^{(k)} \geq 0$ for all $k \geq 1$) is preserved both by (11) and its inverse. For (not necessarily completely monotone) nonnegative ψ, φ satisfies this property for $k \leq d/2+1$. However, for $d = 3$ the properties $\varphi > 0$, $\varphi' < 0$, $\varphi'' > 0$ are not sufficient for a nonnegative ψ. The example, $\varphi(g) = e^{-g}(1 - c\sin g)$ with $|c| < 1/2$ satisfies the above sign conditions. Evaluation of (13) with $d = 3$ by numerical integration shows that for c close to $1/2$ the kinetic profile takes negative values. For odd d a complete characterization of the sets of functions φ determined by (11) with nonnegative ψ is missing.*

5 Solutions of the 3D Euler equations

A large set of solutions $(\rho, \mathbf{u}, T)$ of the 3D Euler equations is given by setting

$$\rho(t,\mathbf{x}) = -\alpha(t)^{-3/2} \varphi'(g(t,\mathbf{x})) \,, \quad T(t,\mathbf{x}) = -\frac{\varphi(g(t,\mathbf{x}))}{\alpha(t)\varphi'(g(t,\mathbf{x}))} \,,$$

with an arbitrary function φ and choosing α, g, and $\mathbf{u}$ according to (7), (9), and (10), respectively. Different qualitative behaviours are obtained for the normal forms of (7), (9), and (10), derived in Section 2.

We start by discussing solutions with finite total mass

$$M = \int_{\mathbb{R}^3} \rho \, d\mathbf{x}$$

and energy

$$E = \int_{\mathbb{R}^3} \left(\frac{3}{2} \rho T + \rho \frac{|\mathbf{u}|^2}{2} \right) d\mathbf{x} \,.$$

Since the x-dependence of the density and the temperature is only through the quadratic form g, it is easily seen that finite values of M and E can only be achieved if g is positive definite, i.e., for the normal form type 3a, with $\lambda^2 < 1 = c$. We then have

$$\alpha(t) = t^2 + 1 \,, \qquad g(t, \mathbf{x}) = \frac{x_1^2 + (1 - \lambda^2)(x_2^2 + x_3^2)}{2(t^2+1)} \,,$$

$$\mathbf{u}(t, \mathbf{x}) = \frac{t\mathbf{x} + \mathbf{x} \times \mathbf{L}}{t^2 + 1} \,, \qquad \text{with } \mathbf{L} = (\lambda, 0, 0) \,.$$

The velocity contains a contribution which is contracting towards the origin for negative t and expanding for positive t and a contribution rotating around the x_1-axis. The level sets of g (and, thus, of ρ and T) are (contracting and expanding) disc shaped ellipsoids, where the flattening is due to the rotational part of the velocity. A straightforward computation gives

$$M = \frac{2\pi\sqrt{2}}{1 - \lambda^2} \int_0^\infty \varphi(\xi) \frac{d\xi}{\sqrt{\xi}} \,, \qquad E = \frac{2\pi\sqrt{2}}{1 - \lambda^2} \left(1 + \frac{2}{1 - \lambda^2} \right) \int_0^\infty \varphi(\xi) \sqrt{\xi} \, d\xi \,,$$

under the assumption that the integrals exist. The internal energy is given by

$$E_i(t) = \frac{3}{2} \int_{\mathbb{R}^3} \rho T \, d\mathbf{x} = \frac{6\pi\sqrt{2}}{(t^2 + 1)(1 - \lambda^2)} \int_0^\infty \varphi(\xi) \sqrt{\xi} \, d\xi \,.$$

As expected (see [2]), it decays like t^{-2} as $t \to \infty$.

Interesting choices of the profile φ include

- the exponential $\varphi(g) = e^{-g}$, giving a spatially constant temperature and an 'ellipsoidal Gaussian' for the density,
- profiles with $\varphi(g) = 0$ for $g \geq g_0$, giving solutions with compact ellipsoidal spatial support contracting and expanding with time,
- profiles with jumps in φ', giving contact discontinuities along certain level sets of $g(t, \mathbf{x})$,
- as an example combining both the previous cases: $\varphi(g) = \max\{0, 1 - g\}$, giving a constant density inside the 1-level set of $g(t, \mathbf{x})$, and vacuum outside.

Of course it is an interesting question if these profiles can be derived from a kinetic profile ψ. It is easily seen that the exponential φ corresponds to an exponential ψ. A smooth φ with compact support corresponds to a ψ with compact support. Lemma 4.1 shows that macroscopic profiles derived from continuous microscopic profiles are in $C^2(\mathbb{R})$ meaning that a profile φ with jumps in the first derivative does not correspond to a regular kinetic profile ψ.

Another interesting class of solutions corresponds to type 3a with $c = -1$, i.e.,

$$\alpha(t) = |t^2 - 1|\,, \qquad g(t, \mathbf{x}) = -\frac{x_1^2 + (1+\lambda^2)(x_2^2 + x_3^2)}{2|t^2-1|}\,,$$
$$\mathbf{u}(t, \mathbf{x}) = \frac{t\mathbf{x} + \mathbf{x} \times \mathbf{L}}{t^2 - 1}\,, \qquad \text{with } \mathbf{L} = (\lambda, 0, 0)\,.$$

Again, bounded total mass is possible,

$$M = \frac{2\pi\sqrt{2}}{1+\lambda^2} \int_0^\infty [\varphi(-\infty) - \varphi(-\xi)] \frac{d\xi}{\sqrt{\xi}}\,,$$

but the total energy is necessarily infinite. The level sets are now cigar shaped ellipsoids, where again the distortion compared to a sphere is caused by rotation.

The main difference to case A is that these solutions are not eternal. Actually, the time intervals $(-\infty, -1)$, $(-1, 1)$, and $(1, \infty)$ should be considered separately. The singularities at $t = \pm 1$ are of concentration type. The three time intervals correspond to

- a solution originating from a spread out state and concentrating at $t = -1$,
- a solution coming out of a concentrated state at $t = -1$ and concentrating again after finite time at $t = 1$, and
- a solution coming out of a concentrated state at $t = 1$ and spreading out as $t \to \infty$.

Note that, for smooth φ these solutions correspond to completely harmless equilibrium solutions of the cometary flow equation, which are smooth at $t = \pm 1$. They just loose their integrability with respect to the velocity at these two instants. Thus, the kinetic solution can be continued smoothly through $t = \pm 1$. This provides a connection between the three time intervals above, which is, however, questionable if only the Euler equations are considered.

Singularities at $t = 0$ with the same qualitative behaviour are featured by solutions of type 3b. We omit a detailed discussion.

All other solution types have infinte total mass and energy. Type 2a solutions concentrate along the x_1-axis at $t = 0$. The set of type 2b solutions contains (with $A_1 = 0$) the only nontrivial steady state solutions (with a purely rotational velocity). Finally, type 0 solutions have the form of planar waves, except type 0a with $B_1 = 0$, leading to

$$\rho = \frac{a}{t^3}, \qquad T = \frac{b}{t^2}, \qquad \mathbf{u} = \frac{\mathbf{x}}{t},$$

with arbitrary constants a and b.

References

[1] C. Cercigniani, *Equilibrium States and trend to Equilibrium in a Gas According to the Boltzmann Equation*, Rendi. Mat. Appl. **10** (1990), pp. 77–95

[2] J. Chemin, *Dynamique des gaz á masse totale finie.* Asymp. Anal. **3** (1990), pp. 215–220.

[3] P. Degond and P.F. Peyrard, *Un modéle de collisions ondes-particules en physique des plasmas: application à la dynamique des gaz*, C. R. Acad. Sci. Paris **323** (1996), pp. 209–214.

[4] P. Degond, J.L. Lopez and P.F. Peyrard, *On the macroscopic dynamics induced by a model wave-particle collision operator*, J. Cont. Mech. Therm. **10** (1998), pp. 153–178.

[5] P. Degond, J.L. Lopez, F. Poupaud and C. Schmeiser, *Existence of solutions of a kinetic equation modelling cometary flows*, J. Stat. Phys. **96** (1999), pp. 361–376.

[6] L. Desvillettes, *Convergence to equilibrium in large time for Boltzmann and B.G.K. equations*, Arch. Rat. Mech. Analysis **110** (1990), pp. 73–91.

[7] J.Earl, J.R. Jokipii and G. Morfill, *Cosmic ray viscosity*, The Astrophysical Journal **331** (1988), L91.

[8] K. Fellner, F. Poupaud and C. Schmeiser, *Existence and convergence to equilibrium of a kinetic equation for cometary flows*, J. Stat. Phys. **114** (2004), pp. 1481–1499.

[9] R. Miller, Nonlinear Volterra integral equations. Mathematics lecture note series, Benjamin, New York (1971).

[10] L. Saint-Raymond, *Incompressible hydrodynamic limits for a kinetic model of waves-particles interaction*, Asymptot. Anal. **19** (1999), no. 2, 149–183.

[11] D. Serre, *Solutions classiques globales des équations d'Euler pour un fluide parfait compressible.* Ann. Inst. Fourier **47** (1997), pp. 139–153.

[12] L.L. Williams and J.R. Jokipii, *Viscosity and inertia in cosmic-ray transport: effects of an average magnetic field*, The Astrophysical Journal **371** (1991), pp. 639–647.

[13] L.L. Williams and J.R. Jokipii, *A single-fluid, self-consistent formulation of fluid dynamics and particle transport*, The Astrophysical Journal **417** (1993), pp. 725–734.

[14] L.L. Williams, N. Schwadron, J.R. Jokipii and T.I. Gombosi, *A unified transport equation for both cosmic rays and thermal particles*, The Astrophysical Journal **405** (1993), pp. L79–L81.